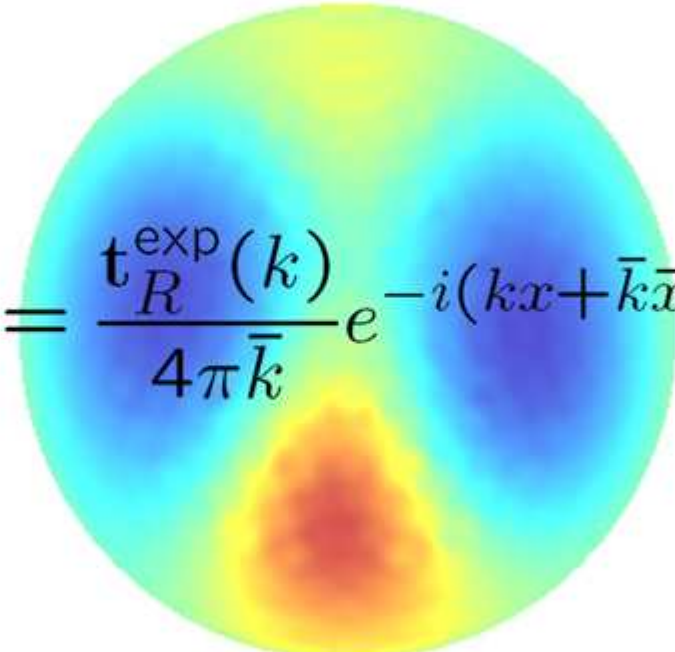


Regularized D-bar method for the inverse conductivity problem

$$\frac{\partial}{\partial \bar{k}} \mu_R(x, k) = \frac{t_R^{\text{exp}}(k)}{4\pi \bar{k}} e^{-i(kx + \bar{k}\bar{x})} \overline{\mu_R(x, k)}$$


Samuli.Siltanen@iki.fi
Tampere University of Technology
Finland

Finnish-Korean Symposium
on Inverse Problems
Seoul, April 2, 2009



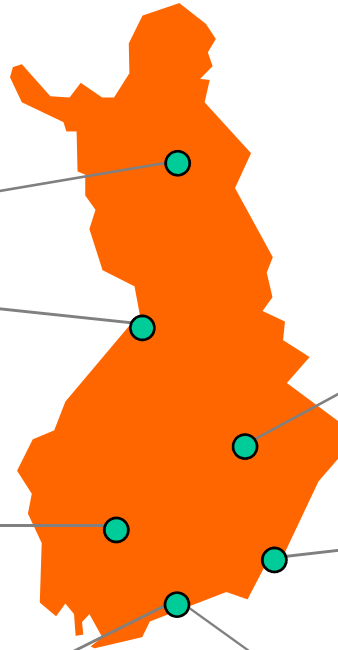
Finnish Centre of Excellence in Inverse Problems Research



TAMPERE UNIVERSITY OF TECHNOLOGY



TEKNILLINEN KORKEAKOULU
TEKNISKA HÖGSKOLAN
HELSINKI UNIVERSITY OF TECHNOLOGY



UNIVERSITY OF KUOPIO



LAPPEENRANTA
UNIVERSITY OF TECHNOLOGY



UNIVERSITY OF HELSINKI

Rolf Nevanlinna Institute

Research institute of mathematics, computer science and statistics

<http://math.tkk.fi/inverse-coe/>

This is a joint work with



David Isaacson

Rensselaer Polytechnic Institute, USA



Kim Knudsen

Technical University of Denmark



Matti Lassas

University of Helsinki, Finland



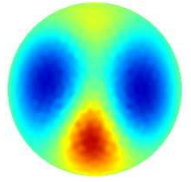
Jennifer Mueller

Colorado State University, USA



Jon Newell

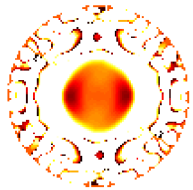
Rensselaer Polytechnic Institute, USA



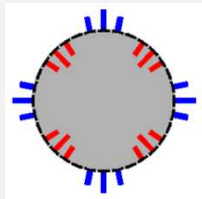
1. The inverse conductivity problem of Calderón



2. Theory of d-bar imaging: infinite precision data



3. Regularized d-bar imaging for noisy data



4. Numerical aspects



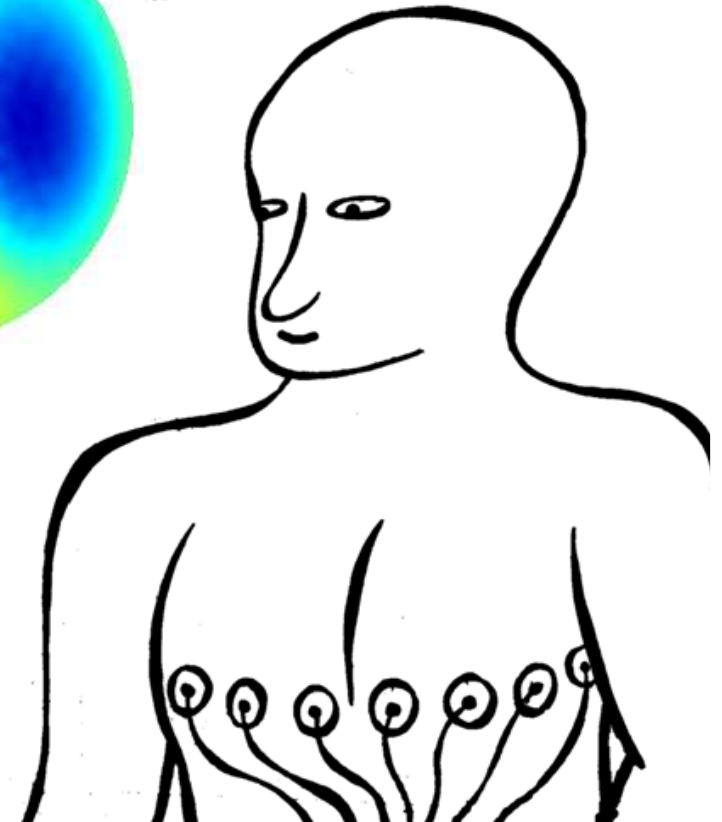
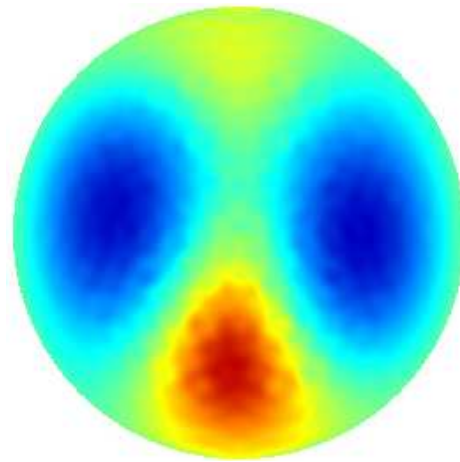
5. Reconstructions

Electrical impedance tomography (EIT) is an emerging medical imaging method

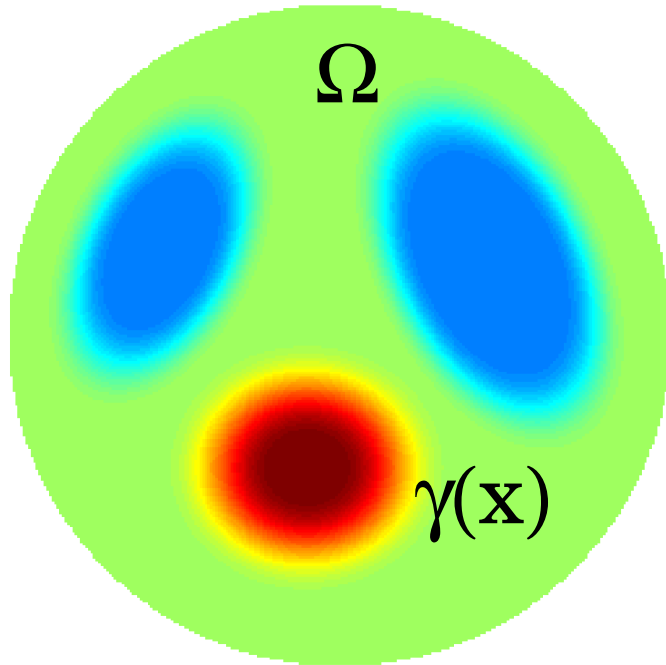
Feed electric currents through electrodes, measure voltages

Reconstruct the image of electric conductivity in a two-dimensional slice

Applications include:
monitoring heart and lungs of unconscious patients,
detecting pulmonary edema,
enhancing ECG and EEG



The inverse conductivity problem of Calderón is the mathematical model of EIT



$$\Lambda_\gamma f = \gamma \frac{\partial u}{\partial \nu} \Big|_{\partial \Omega},$$

$$\begin{aligned} \nabla \cdot \gamma \nabla u &= 0 \quad \text{in } \Omega, \\ u &= f \quad \text{on } \partial \Omega. \end{aligned}$$

We assume that $0 < c \leq \gamma(x) \leq C$ for all $x \in \Omega$.

Problem: given the Dirichlet-to-Neumann map,
how to reconstruct the conductivity?

The reconstruction problem is nonlinear and ill-posed.

EIT reconstruction algorithms can be divided roughly into the following classes:

Linearization (Barber, Bikowski, Brown, Cheney, Isaacson, Mueller, Newell)


Iterative regularization (Dobson, Hua, Kindermann, Lechleiter, Neubauer, Rieder, Rondi, Santosa, Tompkins, Webster, Woo)

Statistical (Bayesian) inversion (Fox, Kaipio, Kolehmainen, Nicholls, Somersalo, Vauhkonen, Voutilainen)

Resistor network methods (Borcea, Druskin, Vasquez)

Convexification (Beilina, Klibanov)

Layer stripping (Cheney, Isaacson, Isaacson, Somersalo)

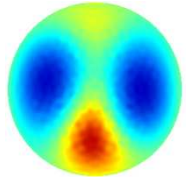
 **The d-bar method** (Astala, Bikowski, Bowerman, Isaacson, Kao, Knudsen, Lassas, Mueller, Murphy, Nachman, Newell, Päivärinta, Saulnier, S, Tamasan)

Teichmüller space methods (Kolehmainen, Lassas, Ola)

Methods for partial information (Alessandrini, Ammari, Bilotta, Brühl, Erhard, Gebauer, Hanke, Hyvönen, Ide, Ikehata, Isozaki, Kang, Kim, Kwon, Lechleiter, Lim, Morassi, Nakata, Potthast, Rossetand, Seo, Sheen, S, Turco, Uhlmann, Wang, and others)

This is a brief history of the d-bar method in 2D

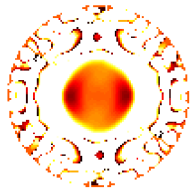
Theory	Practice
1980 Calderón	2008 Bikowski and Mueller
1987 Sylvester and Uhlmann	
1987 R G Novikov	
1988 Nachman	
1996 Nachman	2000 S, Mueller and Isaacson
1997 Liu	2003 Mueller and S
	2004 Isaacson, Mueller, Newell and S
	2006 Isaacson, Mueller, Newell and S
	2007 Murphy
	2008 Knudsen, Lassas, Mueller and S
1997 Brown and Uhlmann	2001 Knudsen and Tamasan
2001 Barceló, Barceló and Ruiz	2003 Knudsen
2000 Francini	
2003 Astala and Päivärinta	2008 Astala, Mueller, Päivärinta and S
2007 Barceló, Faraco and Ruiz	
2008 Clop, Faraco and Ruiz	
2008 Bukhgeim	



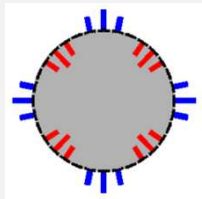
1. The inverse conductivity problem of Calderón



2. Theory of d-bar imaging: infinite precision data



3. Regularized d-bar imaging for noisy data



4. Numerical aspects



5. Reconstructions

Nachman's 1996 proof consists of two steps:

$$\Lambda_\gamma \longrightarrow \mathbf{t} \longrightarrow \gamma$$

The intermediate object \mathbf{t} is a complex-valued function called *scattering transform* and defined as follows:

$$\mathbf{t}(k) := \int_{\mathbb{R}^2} e^{i\bar{k}\bar{x}} q(x) \psi(x, k) dx$$

$$q = \frac{\Delta \gamma^{1/2}}{\gamma^{1/2}}$$

$$(-\Delta + q)\psi(\cdot, k) = 0$$

$$\psi(x, k) \sim e^{ikx} = e^{i(k_1 + ik_2)(x_1 + ix_2)}$$

Step 1: from DN map to scattering transform

Solve traces of ψ from the boundary integral equation

$$\psi(\cdot, k)|_{\partial\Omega} = e^{ikx} - S_k(\Lambda_\gamma - \Lambda_1)\psi(\cdot, k),$$

where the single-layer operator has Faddeev Green's function as kernel.

Compute the scattering transform as

$$\mathbf{t}(k) = \int_{\partial\Omega} e^{i\bar{k}\bar{x}} (\Lambda_\gamma - \Lambda_1)\psi(x, k) d\sigma(x).$$

Let us take a closer look at Faddeev Green's function and the related single layer operator

The operator

$$(S_k\phi)(x) := \int_{\partial\Omega} G_k(x-y)\phi(y)d\sigma(y)$$

involves the Faddeev Green's function G_k for the Laplacian:

$$-\Delta G_k(x) = \delta_0(x).$$

The function G_k can be written in the form

$$G_k(x) := e^{ikx}g_k(x),$$

where

$$g_k(x) := \frac{1}{(2\pi)^2} \int_{\mathbb{R}^2} \frac{e^{ix\cdot\xi}}{|\xi|^2 + 2k(\xi_1 + i\xi_2)} d\xi.$$

Step 2: from scattering transform to γ

Define $\mu(x, k) = e^{-ikx}\psi(x, k)$

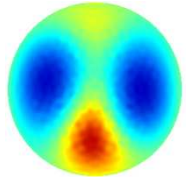
Then the following d-bar equation holds:

$$\frac{\partial}{\partial \bar{k}} \mu(x, k) = \frac{t(k)}{4\pi \bar{k}} e^{-i(kx + \bar{k}\bar{x})} \overline{\mu(x, k)}.$$

Here $\frac{\partial}{\partial \bar{k}} = \frac{1}{2} \left(\frac{\partial}{\partial k_1} + i \frac{\partial}{\partial k_2} \right)$.

The d-bar equation has a unique solution for all x .
The conductivity can be recovered from

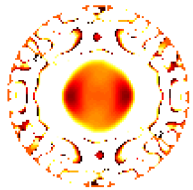
$$\gamma^{1/2}(x) = \lim_{k \rightarrow 0} \mu(x, k).$$



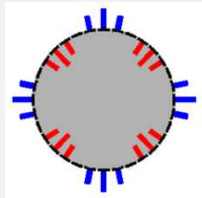
1. The inverse conductivity problem of Calderón



2. Theory of d-bar imaging: infinite precision data



3. Regularized d-bar imaging for noisy data



4. Numerical aspects



5. Reconstructions

We work within the following assumptions:

Let $\Omega \subset \mathbb{R}^2$ be the open unit disc.

Define the forward map F between the spaces

$$F : \mathcal{D}(F) \subset L^\infty(\Omega) \rightarrow Y.$$

Domain $\mathcal{D}(F)$ is defined as follows.

Let $M > 0$ and $0 < \rho < 1$. The set $\mathcal{D}(F)$ contains functions $\gamma : \Omega \rightarrow \mathbb{R}$ satisfying

$$(a) \|\gamma\|_{C^2(\overline{\Omega})} \leq M,$$

$$(b) \gamma(x) \geq M^{-1} \text{ for all } x \in \Omega,$$

$$(c) \gamma(x) \equiv 1 \text{ for } \rho < |x| < 1.$$

Space Y of data is defined as follows.

Y consists of bounded linear operators

$$\Lambda : H^{1/2}(\partial\Omega) \rightarrow H^{-1/2}(\partial\Omega)$$

satisfying $\int_{\partial\Omega} \Lambda(f) d\sigma = 0$ and $\Lambda(1) = 0$.

Let us emphasize one of the strengths of our new results

Conditional stability results have the form

$$\|\gamma_1 - \gamma_2\|_Z \leq f(\|\Lambda_{\gamma_1} - \Lambda_{\gamma_2}\|_Y),$$

where γ_1, γ_2 belong to some function space Z and f is a continuous function with $f(0) = 0$.

The above estimate is not practically relevant.

The noisy measurement $\Lambda_{\gamma}^{\varepsilon}$ is in general not the DN map of some conductivity.

In contrast, we prove regularization properties for the D-bar method under the practically feasible assumption $\|\Lambda_{\gamma}^{\varepsilon} - \Lambda_{\gamma}\|_Y \leq \varepsilon$.

Let us define nonlinear regularization strategy

(following Engl, Hanke & Neubauer and Kirsch)

Recall direct problem: $\gamma \in X$ maps to $\Lambda_\gamma \in Y$.

A family of continuous mappings $\Gamma_\alpha : Y \rightarrow X$ with $0 < \alpha < \infty$ is a **regularization strategy** if

$$\lim_{\alpha \rightarrow 0} \|\Gamma_\alpha \Lambda_\gamma - \gamma\|_{L^\infty(\Omega)} = 0$$

for each fixed $\gamma \in X$. A regularization strategy with a choice $\alpha = \alpha(\varepsilon)$ is called **admissible** if

$$\alpha(\varepsilon) \rightarrow 0 \text{ as } \varepsilon \rightarrow 0,$$

and for any fixed $\gamma \in X$ the following holds:

$$\sup_{\Lambda_\gamma^\varepsilon} \left\{ \|\Gamma_{\alpha(\varepsilon)} \Lambda_\gamma^\varepsilon - \gamma\|_{L^\infty(\Omega)} : \|\Lambda_\gamma^\varepsilon - \Lambda_\gamma\|_Y \leq \varepsilon \right\} \xrightarrow{\varepsilon \rightarrow 0} 0.$$

This is our regularized D-bar method for EIT

Given the noise level $\varepsilon > 0$, solve the equation

$$\psi^\varepsilon(\cdot, k)|_{\partial\Omega} = e^{ikx} - S_k(\Lambda_\gamma^\varepsilon - \Lambda_1)\psi^\varepsilon(\cdot, k)|_{\partial\Omega}$$

for $|k| < R(\varepsilon) := -\frac{1}{10} \log(\varepsilon)$.

Introduce nonlinear low-pass filtering

$$\mathbf{t}_R^\varepsilon(k) := \begin{cases} \int_{\partial\Omega} e^{i\bar{k}\bar{x}} (\Lambda_\gamma^\varepsilon - \Lambda_1)\psi^\varepsilon(\cdot, k) d\sigma & \text{for } |k| < R(\varepsilon), \\ \text{zero} & \text{for } |k| \geq R(\varepsilon). \end{cases}$$

For each $x \in \Omega$, solve the integral equation

$$\mu_R(x, k) = 1 + \frac{1}{(2\pi)^2} \int_{\mathbb{R}^2} \frac{\mathbf{t}_R^\varepsilon(s)}{(k-s)\bar{s}} e^{-x(s)} \overline{\mu_R(x, s)} ds_1 ds_2,$$

and define $\alpha(\varepsilon) = \frac{1}{R(\varepsilon)}$ and $(\Gamma_\alpha \Lambda_\gamma^\varepsilon)(x) := (\mu_R(x, 0))^2$.

Theorem [Knudsen, Lassas, Mueller & S 2008]

The family Γ_α is well-defined for small $\alpha > 0$. It is an admissible regularization strategy with

$$\alpha(\varepsilon) = \left(-\frac{1}{10} \log(\varepsilon)\right)^{-1}.$$

Furthermore, we have the explicit estimate

$$\sup_{\Lambda_\gamma^\varepsilon} \left\{ \|\Gamma_{\alpha(\varepsilon)} \Lambda_\gamma^\varepsilon - \gamma\|_{L^\infty(\Omega)} : \|\Lambda_\gamma^\varepsilon - \Lambda_\gamma\|_Y \leq \varepsilon \right\}$$

$$\leq C(-\log \varepsilon)^{-1/14}$$

$$\rightarrow 0 \text{ as } \varepsilon \rightarrow 0.$$

Proof of the main theorem is divided into several lemmata. First a D-bar estimate:

Lemma 1. Let $4/3 < r_0 < 2$ and suppose that $\phi_1, \phi_2 \in L^r(\mathbb{R}^2)$ for all $r \geq r_0$. Let μ_1, μ_2 , be the solutions of

$$\mu_j(x, k) = 1 + \frac{1}{(2\pi)^2} \int_{\mathbb{R}^2} \frac{\phi_j(k')}{(k - k')} \overline{\mu_j(x, k')} dk'_1 dk'_2,$$

$j = 1, 2$. Then for fixed $x \in \overline{\Omega}$ we have

$$\|\mu_1(x, \cdot) - \mu_2(x, \cdot)\|_{C^\alpha(\mathbb{R}^2)} \leq C \|\phi_1 - \phi_2\|_{L^{r_0} \cap L^{r_0'}(\mathbb{R}^2)},$$

where $\alpha < 2/r_0 - 1$ and $1/r_0' = 1 - 1/r_0$.

Proof. Combination of well-known results.

These results follow from careful analysis of Faddeev's Green function

Lemma 2. Let $\phi_0 \in H^{-1/2}(\partial\Omega)$ with $\int \phi_0 = 0$. Then we have the estimate

$$\|S_k \phi_0\|_{H^{1/2}(\partial\Omega)} \leq C e^{2|k|} (1 + |k|) \|\phi_0\|_{H^{-1/2}(\partial\Omega)}.$$

Lemma 3. For $k \in \mathbb{C}$ we have the estimate

$$\left\| [I + S_k(\Lambda_\gamma - \Lambda_1)]^{-1} \right\|_{L(H^s(\partial\Omega))} \leq C_2 e^{2|k|} (1 + |k|),$$

where C_2 depends only on M and ρ .

Combining previous results, a perturbation argument, and delicate L^p analysis shows

Lemma 4. There exists $\varepsilon_0 > 0$, depending only on M and ρ , such that equation

$$\psi^\varepsilon(\cdot, k)|_{\partial\Omega} = e^{ikx} - S_k(\Lambda_\gamma^\varepsilon - \Lambda_1)\psi^\varepsilon(\cdot, k)|_{\partial\Omega}$$

is solvable in $H^{1/2}(\partial\Omega)$ for all $0 < \varepsilon \leq \varepsilon_0$ and $|k| < R$ with

$$R = R(\varepsilon) = -\frac{1}{10} \log \varepsilon.$$

Furthermore, for $p > 1$ we have the estimate

$$\left\| \frac{\mathbf{t}(k) - \mathbf{t}_R^\varepsilon(k)}{\bar{k}} \right\|_{L^p(|k| \leq R)} \leq C \varepsilon^{1/10} \left(-\frac{1}{10} \log \varepsilon \right)^{2/p},$$

where C is independent of p and R and ε .

Sketch of proof of main theorem

(i) $\lim_{\alpha \rightarrow 0} \|\Gamma_\alpha \Lambda_\gamma - \gamma\|_{L^\infty(\Omega)} = 0$ for $\gamma \in X$.

(ii) $\alpha(\varepsilon) \rightarrow 0$ as $\varepsilon \rightarrow 0$,

(iii) $\sup_{\Lambda_\gamma^\varepsilon} \left\{ \|\Gamma_{\alpha(\varepsilon)} \Lambda_\gamma^\varepsilon - \gamma\|_{L^\infty(\Omega)} : \|\Lambda_\gamma^\varepsilon - \Lambda_\gamma\|_Y \leq \varepsilon \right\}$
tends to zero as $\varepsilon \rightarrow 0$.

Claim (i) follows from [Nachman 1996] (with delicate choices of L^p spaces) and Lemma 1.
Claim (ii) is OK: $\alpha(\varepsilon) = \frac{1}{R(\varepsilon)} = -10(\log \varepsilon)^{-1}$.

Sketch of proof of main theorem

To prove that

$$\sup_{\Lambda_\gamma^\varepsilon} \left\{ \|\Gamma_{\alpha(\varepsilon)} \Lambda_\gamma^\varepsilon - \gamma\|_{L^\infty(\Omega)} : \|\Lambda_\gamma^\varepsilon - \Lambda_\gamma\|_Y \leq \varepsilon \right\}$$

tends to zero as $\varepsilon \rightarrow 0$ we combine [Nachman 1996] with Lemmata 1 and 4 to estimate

$$\begin{aligned} & \|\mu(x, \cdot) - \mu_R(x, \cdot)\|_{C^\alpha(\mathbb{R}^2)} \\ & \leq C \left\| \frac{\mathbf{t}(k) - \mathbf{t}_R^\varepsilon(k)}{\bar{k}} \right\|_{L^p \cap L^{p'}(\mathbb{R}^2)} \\ & \leq C \left\| \frac{\mathbf{t}(k) - \mathbf{t}_R^\varepsilon(k)}{\bar{k}} \right\|_{L^p \cap L^{p'}(|k| < R)} + C \left\| \frac{\mathbf{t}(k)}{\bar{k}} \right\|_{L^p(|k| > R)} \\ & \leq C \left(-\frac{1}{10} \log \varepsilon\right)^{10/7} \varepsilon^{1/10} + CR(\varepsilon)^{-\frac{1}{7}} + CR(\varepsilon)^{-\frac{1}{14}} \\ & = C(-\log \varepsilon)^{10/7} \varepsilon^{1/10} + C(-\log \varepsilon)^{-\frac{1}{7}} + C(-\log \varepsilon)^{-\frac{1}{14}}. \end{aligned}$$

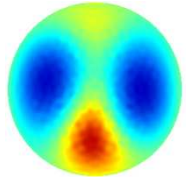
One more thing: the regularization strategy is not yet defined on all of data space Y

The range $F(\mathcal{D}(F)) \subset Y$ is not known, and its structure may be complicated.

(This is related to the open and notoriously difficult *characterization problem*.)

The previous results show the claim only for operators ε_0 -close to the range $F(\mathcal{D}(F))$.

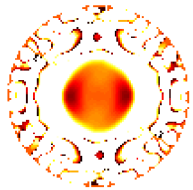
The problem can be overcome using spectral theoretical arguments.



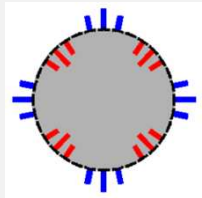
1. The inverse conductivity problem of Calderón



2. Theory of d-bar imaging: infinite precision data



3. Regularized d-bar imaging for noisy data

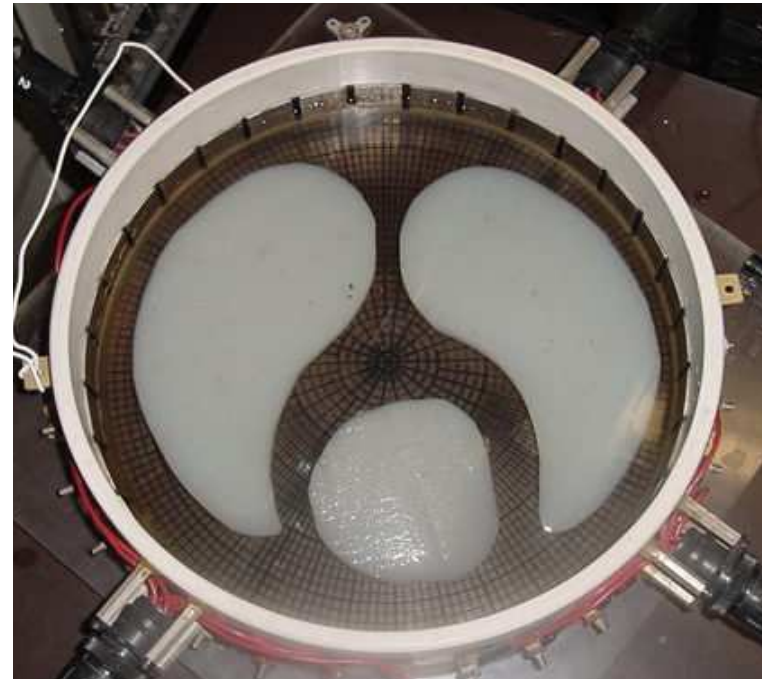
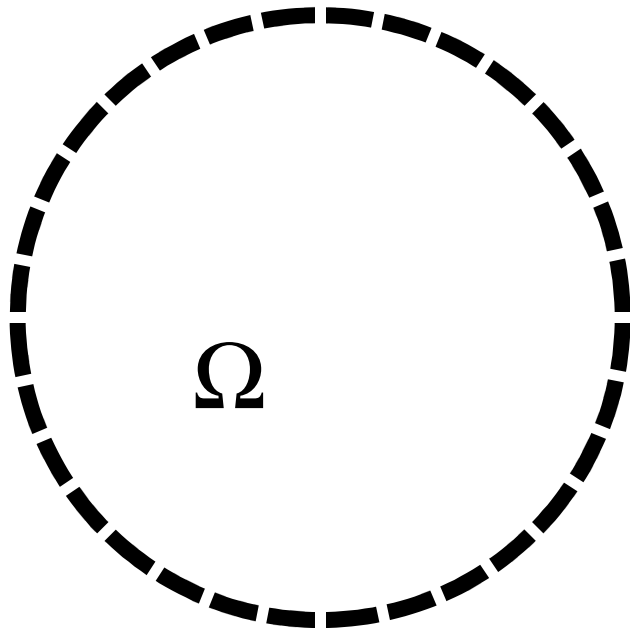


4. Numerical aspects



5. Reconstructions

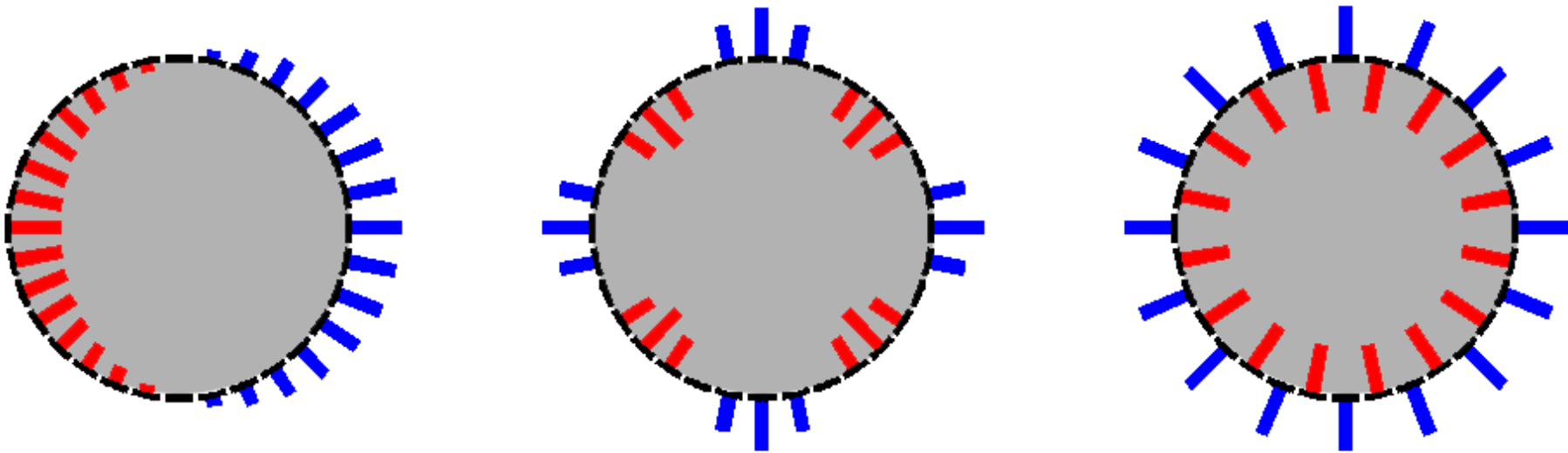
**Practical measurements use electrodes.
Here is a typical arrangement:**



The number of electrodes here is $N=32$.
The device is in Rensselaer Polytechnic Institute, New York, USA.

A linearly independent set of current patterns is fed into the domain and voltages measured

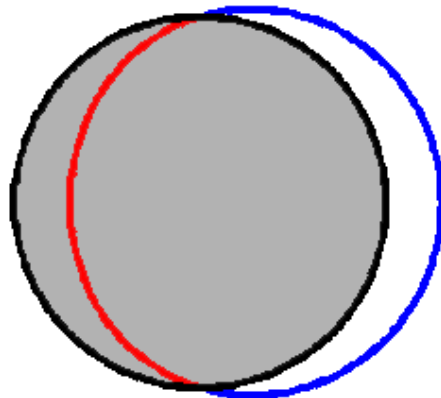
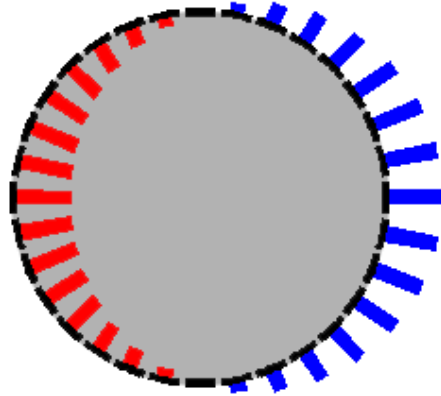
Three examples of current patterns in the case $N=32$:



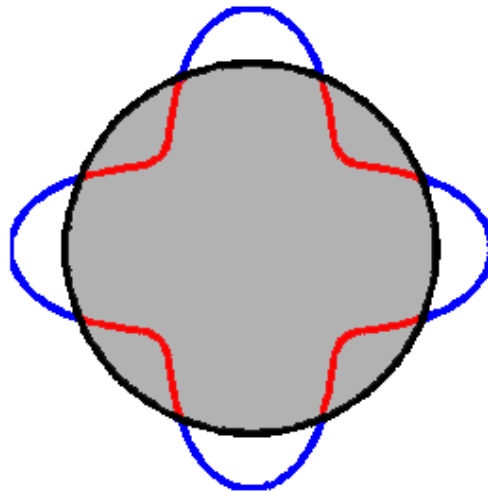
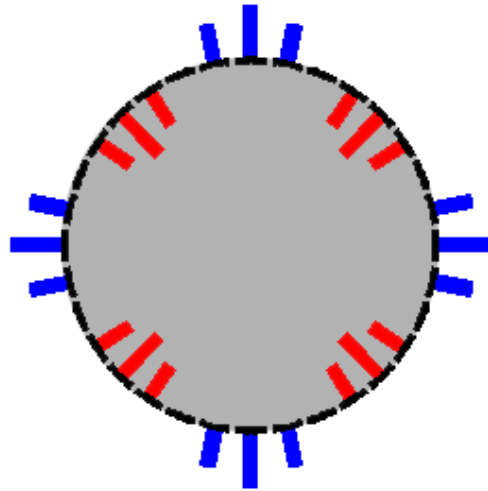
Conservation of charge dictates that there are $N-1$ linearly independent current patterns.

Discrete current patterns approximate trigonometric basis functions at the boundary

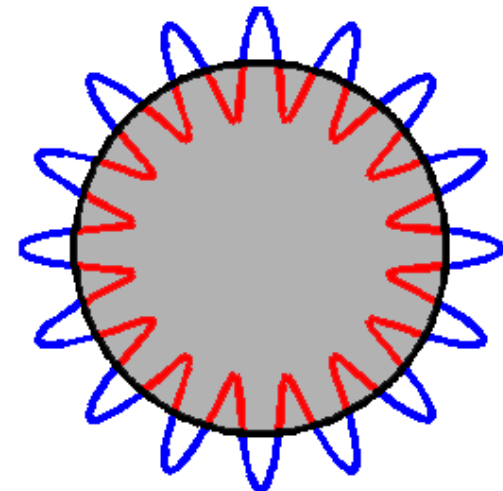
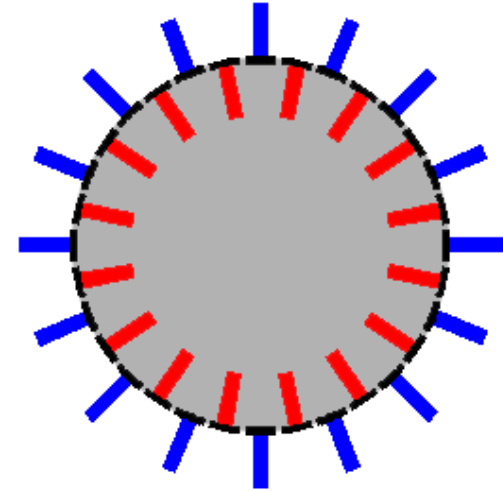
$\cos(\theta)$



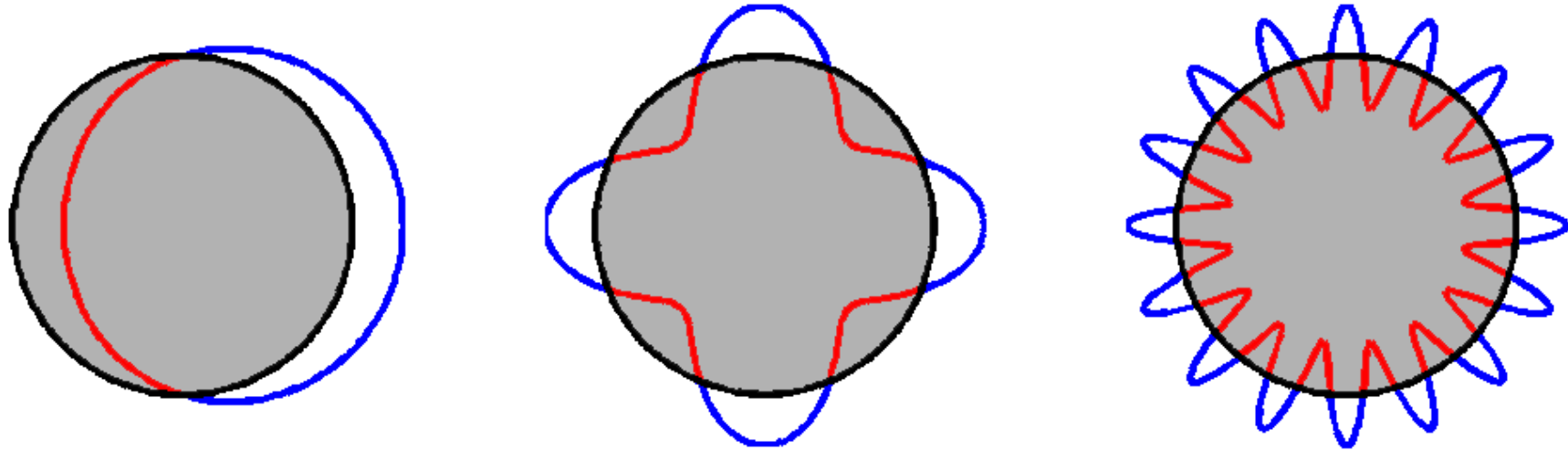
$\cos(4\theta)$



$\cos(16\theta)$



We use the truncated Fourier basis $\{e^{in\theta}\}_{n=-N}^N$ to express functions defined on the unit circle.



Integral operators $A : H^s(\partial\Omega) \rightarrow H^r(\partial\Omega)$ are represented as finite matrices $[\langle Ae^{in\theta}, e^{im\theta} \rangle]$.

- Λ_1 we know analytically,
- Λ_γ we compute using Finite Element Method,
- S_k we evaluate by numerical integration.

This is our practical two-step regularized D-bar method for EIT

1. We solve for $|k| < R$ the matrix version of

$$\psi^\varepsilon(\cdot, k)|_{\partial\Omega} = e^{ikx} - S_k(\Lambda_\gamma^\varepsilon - \Lambda_1)\psi^\varepsilon(\cdot, k)|_{\partial\Omega}$$

with R as large as numerically stable.

2. The integral equation

$$\mu_R(x, k) = 1 + \frac{1}{(2\pi)^2} \int_{\mathbb{R}^2} \frac{t_R^\varepsilon(s)}{(k-s)\bar{s}} e^{-x(s)} \overline{\mu_R(x, s)} ds_1 ds_2$$

can be solved by our established D-bar solver.

The reconstructed conductivity is $\mu_R(x, 0)$.

The d-bar equation is written in integral form for easier numerical solution

Write the d-bar equation

$$\frac{\partial}{\partial \bar{k}} \mu_R(x, k) = \frac{t_R(k)}{4\pi \bar{k}} e^{-i(kx + \bar{k}x)} \overline{\mu_R(x, k)}$$

in integral form using the appropriate Green function:

$$\mu_R(x, k) = 1 + \frac{1}{\pi k} * \left(\frac{t_R(k)}{4\pi \bar{k}} e^{-i(kx + \bar{k}x)} \overline{\mu_R(x, k)} \right).$$

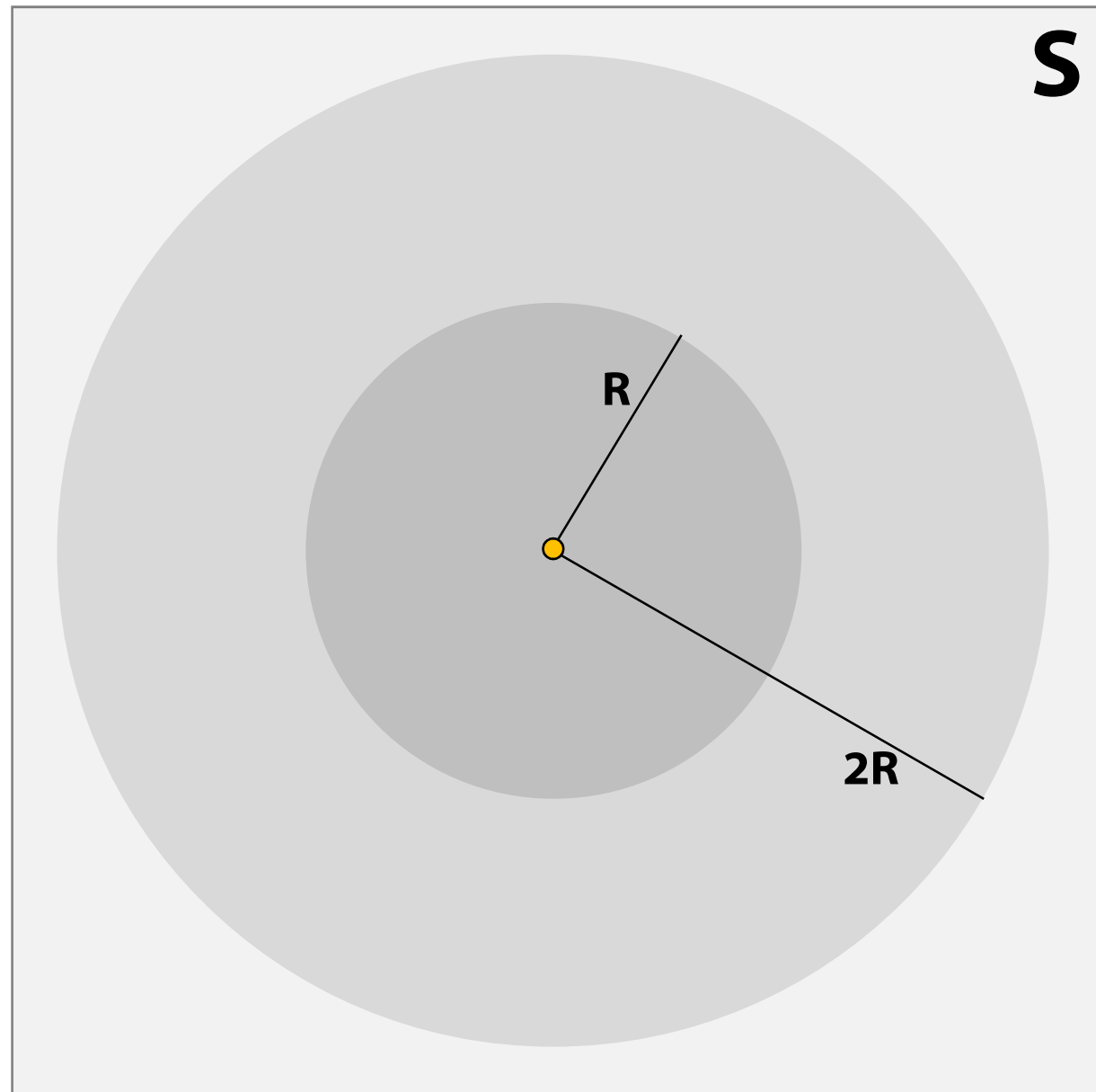
This equation of the Lippmann-Schwinger form can be solved numerically as explained below. Then

$$\gamma_R^{1/2}(x) = \mu_R(x, 0).$$

The \bar{d} equation is defined on the whole k -plane.

However, numerical solution requires a finite computational domain.

To this end, we consider periodic functions. The plane is tiled by the square $S = [-2R - \epsilon, 2R + \epsilon]^2$.



We introduce an S -periodic version of the d -bar equation.

Green's functions $g : \mathbb{C} \rightarrow \mathbb{C}$ and $\tilde{g} : S \rightarrow \mathbb{C}$:

$$g(k) = \frac{1}{\pi k}, \quad \tilde{g}(k) = \frac{1}{\pi k} \Big|_S$$

Denote the multiplier function as follows:

$$T_R(k) = \frac{t_R(k)}{4\pi\bar{k}} e^{-i(kx + \bar{k}\bar{x})},$$

and set $\tilde{T}_R(k) = T_R(k)|_S$. The d -bar equations:

$$\begin{aligned} \mu_R(x, k) &= 1 + \int_{\mathbb{C}} g(k - \lambda) T_R(\lambda) \overline{\mu_R(x, \lambda)} d\lambda \\ \tilde{\mu}_R(x, k) &= 1 + \int_S \tilde{g}(k - \lambda) \tilde{T}_R(\lambda) \overline{\tilde{\mu}_R(x, \lambda)} d\lambda \end{aligned}$$

Now the d-bar equation can be essentially solved in the square S instead of the k -plane.

Green's functions $g : \mathbb{C} \rightarrow \mathbb{C}$ and $\tilde{g} : S \rightarrow \mathbb{C}$:

$$g(k) = \frac{1}{\pi k}, \quad \tilde{g}(k) = \frac{1}{\pi k} \Big|_S$$

Denote the multiplier function as follows:

$$T_R(k) = \frac{t_R(k)}{4\pi\bar{k}} e^{-i(kx + \bar{k}\bar{x})},$$

and set $\tilde{T}_R(k) = T_R(k)|_S$. The d-bar equations:

$$\mu_R(x, k) = 1 + \int_{D(0, R)} g(k - \lambda) T_R(\lambda) \overline{\mu_R(x, \lambda)} d\lambda$$

$$\tilde{\mu}_R(x, k) = 1 + \int_{D(0, R)} \tilde{g}(k - \lambda) \tilde{T}_R(\lambda) \overline{\tilde{\mu}_R(x, \lambda)} d\lambda$$

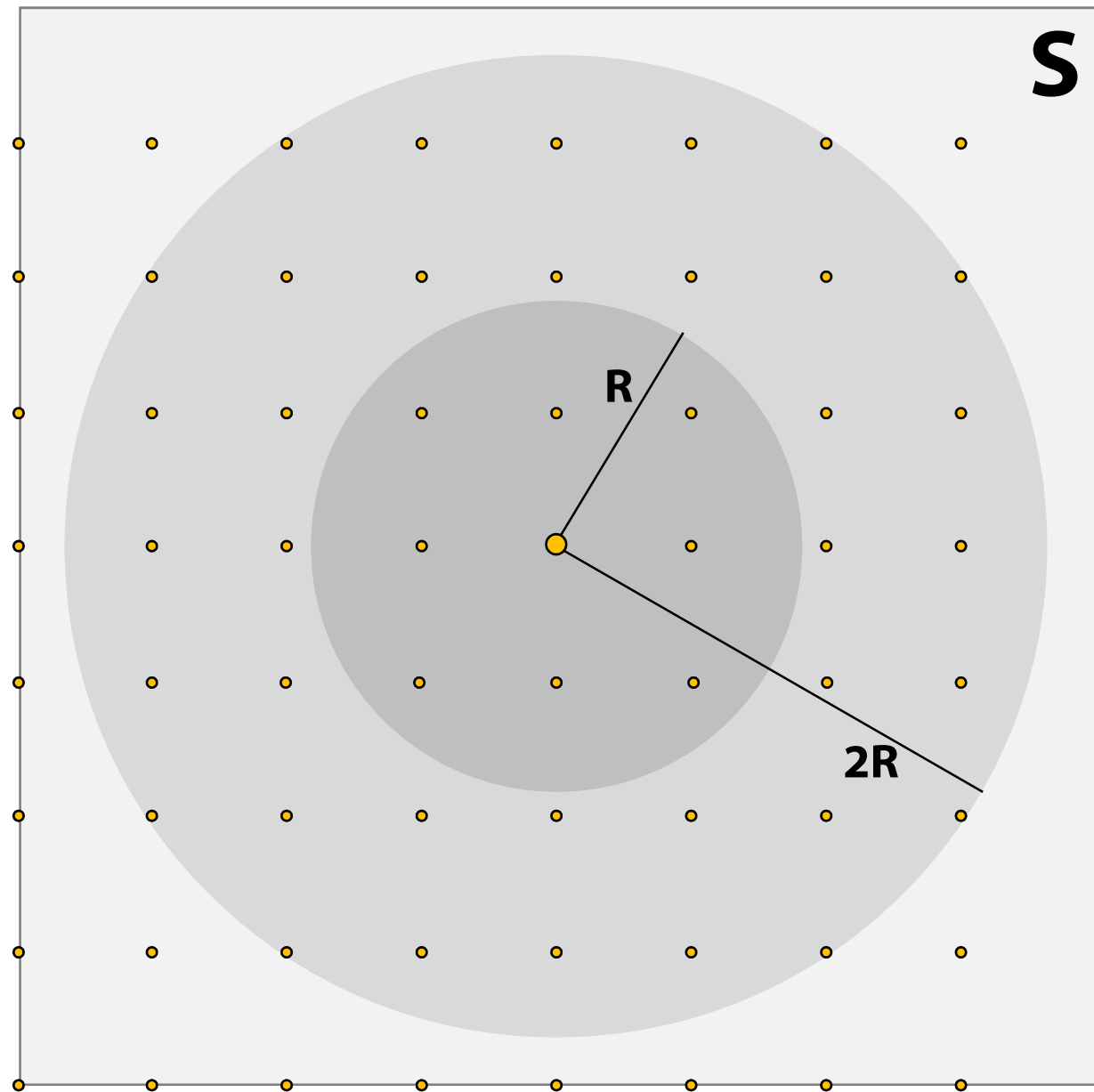
It can be shown that

$$\mu_R(x, k) = \tilde{\mu}_R(x, k) \quad \text{for } |k| < R.$$

We form a grid suitable for FFT (fast Fourier transform).

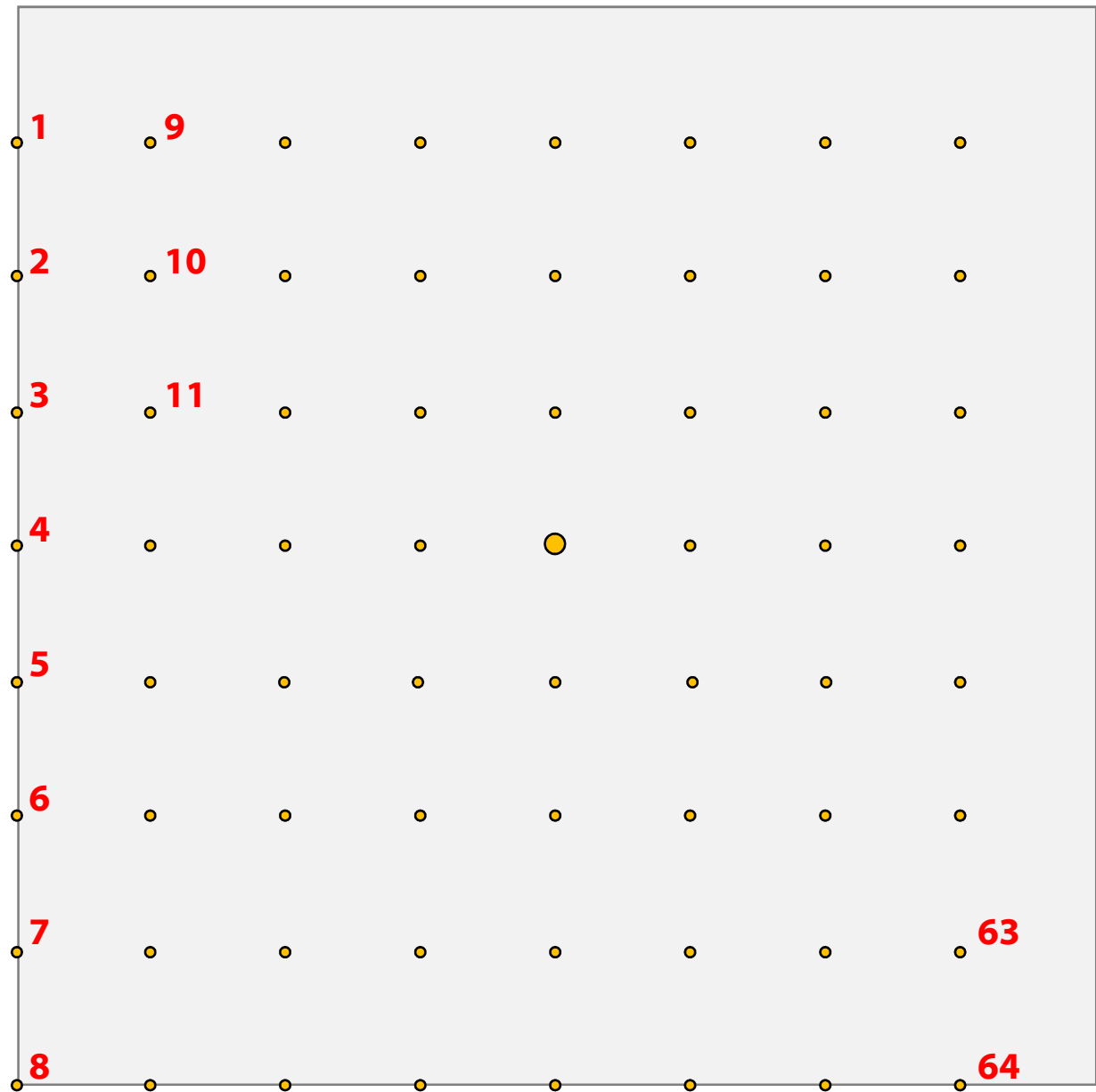
Here 8x8 grid is shown; in practice we typically use 512x512 points.

Periodic functions are represented by their values at the grid points.



Periodic functions are represented by their values at the grid points, real and imaginary parts separately:

$$\begin{bmatrix} \text{Re } \varphi(k_1) \\ \text{Re } \varphi(k_2) \\ \vdots \\ \text{Re } \varphi(k_{64}) \\ \text{Im } \varphi(k_1) \\ \text{Im } \varphi(k_2) \\ \vdots \\ \text{Im } \varphi(k_{64}) \end{bmatrix} \in \mathbb{R}^{128}$$



The solution of the periodic equation is reduced to iterative solution of a linear system

Write the periodic integral equation

$$\tilde{\mu}_R(x, k) = 1 + \int_S \tilde{g}(k - \lambda) \tilde{T}_R(\lambda) \overline{\tilde{\mu}_R(x, \lambda)} d\lambda$$

in the form

$$[I - \tilde{g} * (\tilde{T}_R \cdot -)] \tilde{\mu}_R = 1. \quad (1)$$

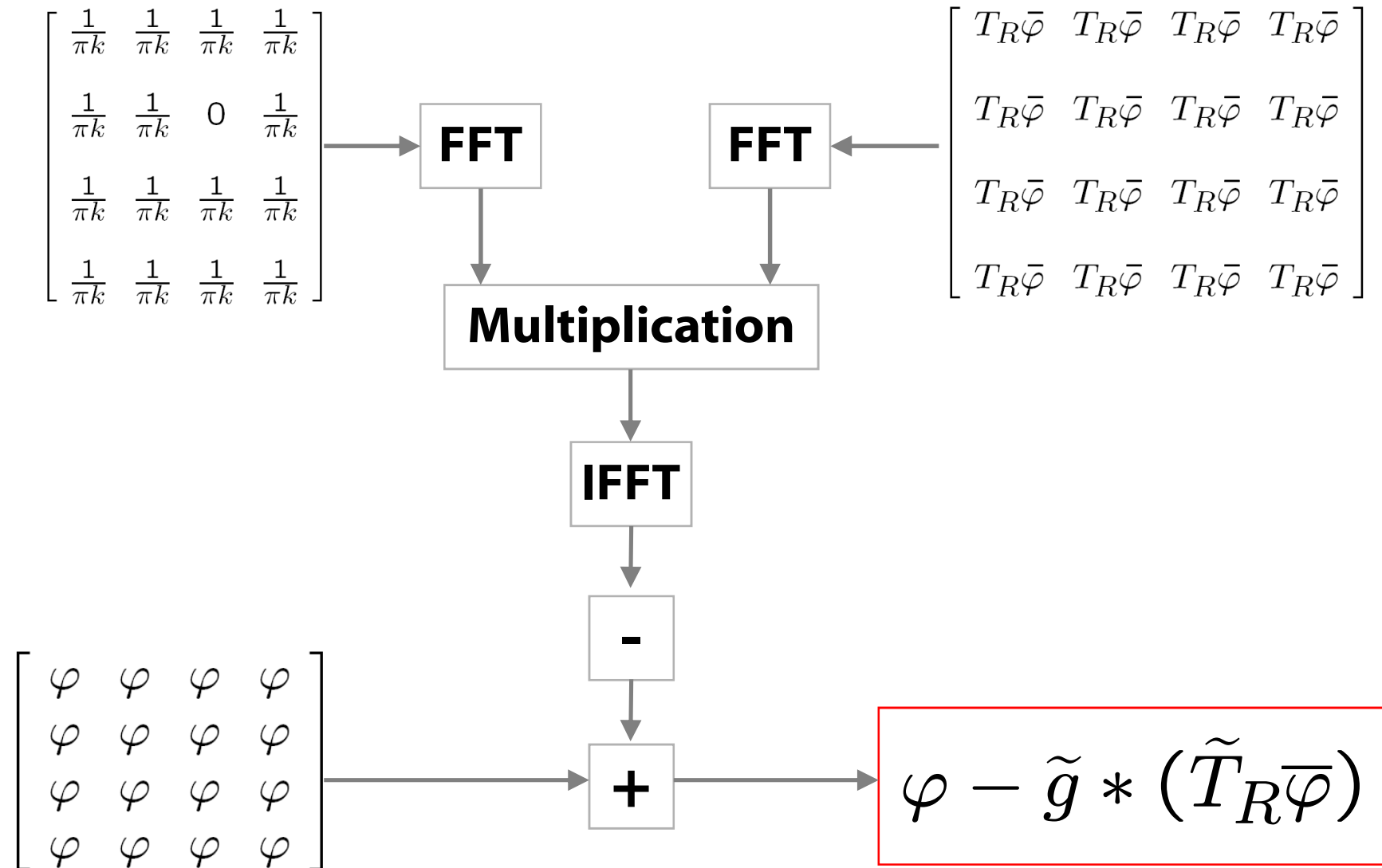
We represent the solution $\tilde{\mu}_R$ as a vector of point values as shown above.

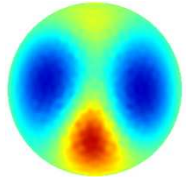
Then we can use an iterative solver, such as GMRES, to solve (1) provided we have a computational routine for the real-linear operation

$$\varphi \mapsto \varphi - \tilde{g} * (\tilde{T}_R \overline{\varphi}).$$

See [Vainikko 2000] and [Knudsen, Mueller and S 2004].

Periodic convolution is conveniently implemented using the FFT

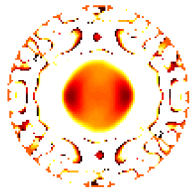




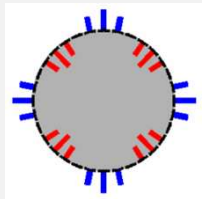
1. The inverse conductivity problem of Calderón



2. Theory of d-bar imaging: infinite precision data



3. Regularized d-bar imaging for noisy data

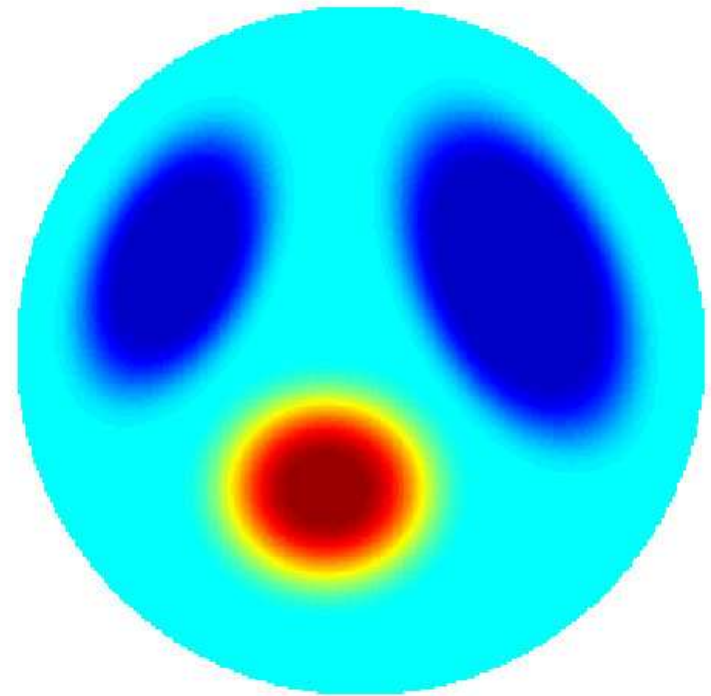
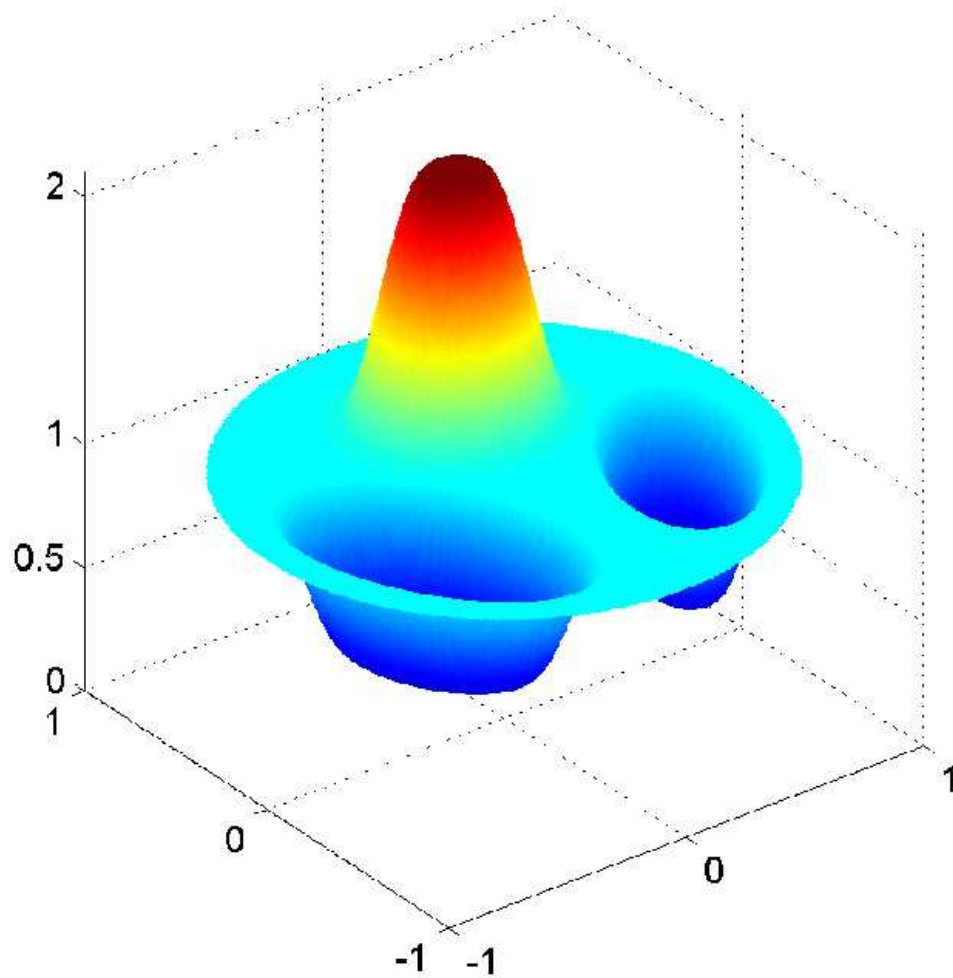


4. Numerical aspects

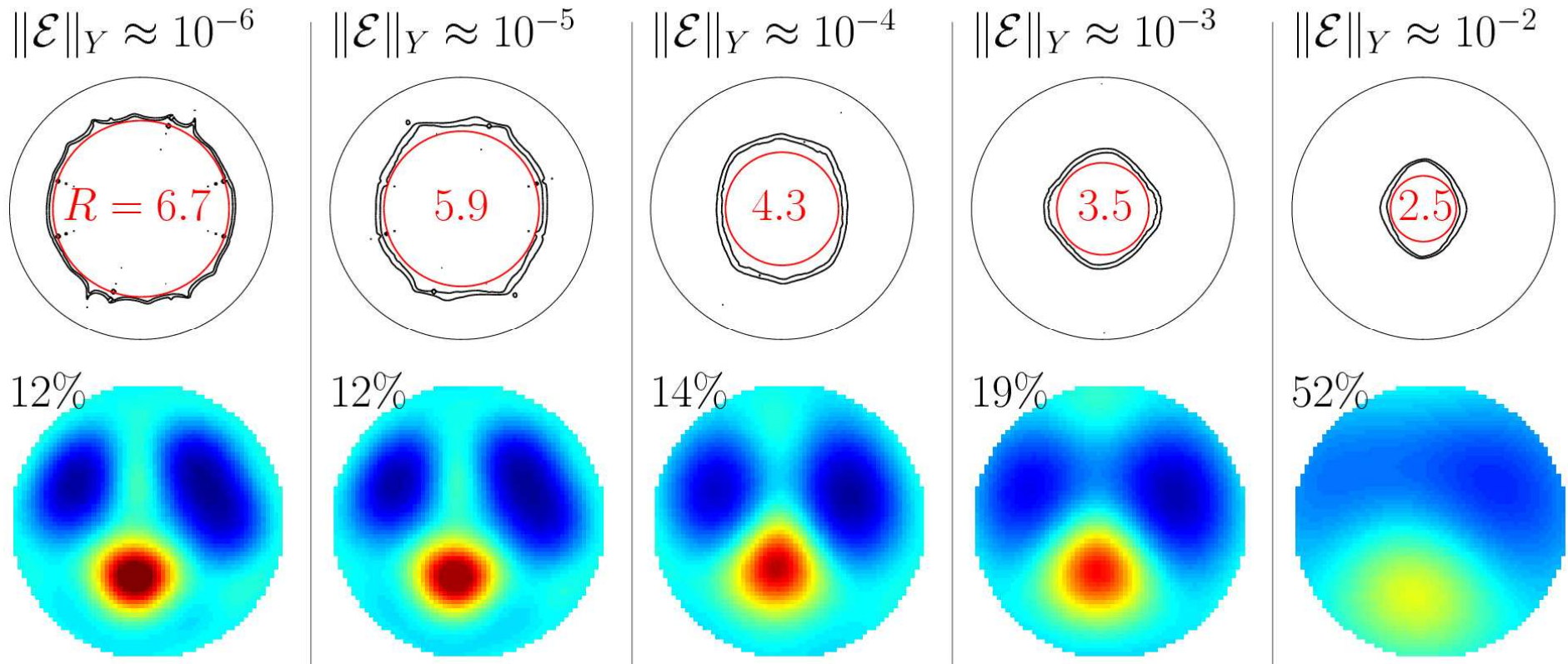


5. Reconstructions

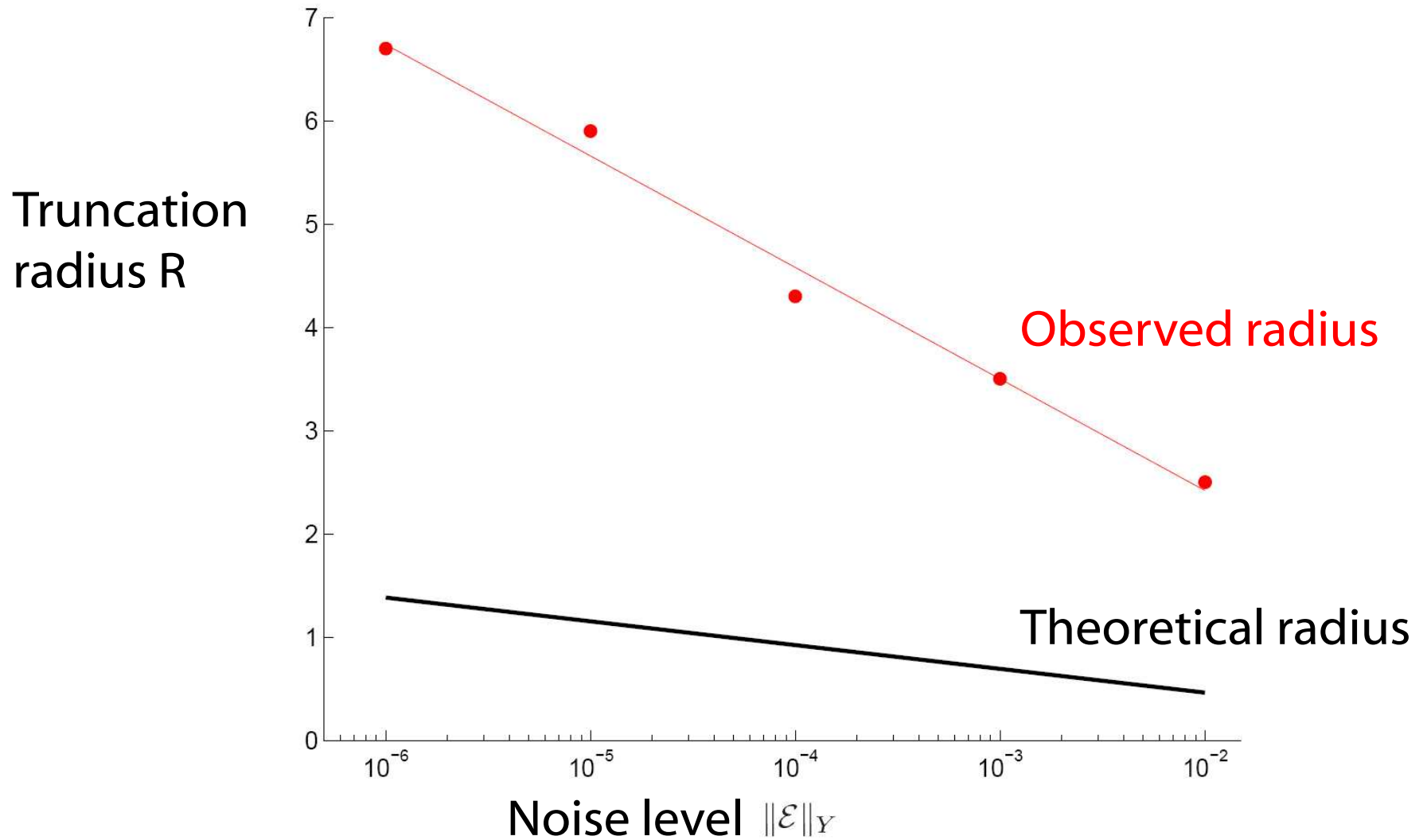
We construct a simulated human chest phantom for numerical testing



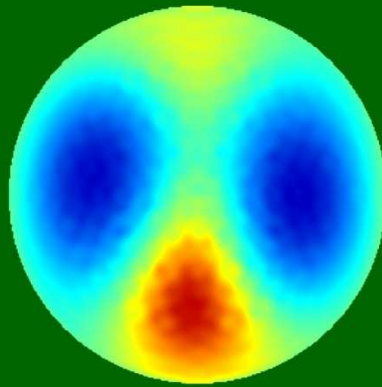
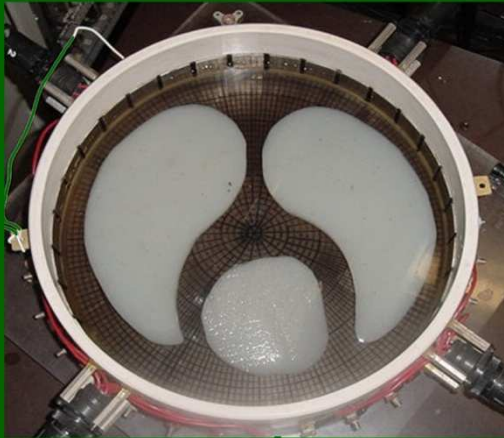
Here we see the reconstructions corresponding to various levels of measurement noise



The numerical results actually improve the exponential behaviour predicted by theory



We have achieved excellent EIT reconstructions from practical data (phantom and *in vivo* human) using Born approximation to linearize Step 1.



However, that approach does not allow regularization analysis.

Thank you!

Preprints available at
www.siltanen-research.net

Knudsen K, Lassas M, Mueller J L and Siltanen S

Reconstructions of Piecewise Constant Conductivities by the D-bar Method for Electrical Impedance Tomography
To appear in proceedings of Applied Inverse Problems 2007, Vancouver.

Knudsen K, Lassas M, Mueller J L and Siltanen S 2007

D-bar method for electrical impedance tomography with discontinuous conductivities
SIAM Journal of Applied Mathematics **67**(3), pp. 893-913

Lassas M, Mueller J L and Siltanen S 2007

Mapping properties of the nonlinear Fourier transform in dimension two
Communications in Partial Differential Equations **32**(4), pp. 591-610

Isaacson D, Mueller J L, Newell J and Siltanen S 2006

Imaging Cardiac Activity by the D-bar Method for Electrical Impedance Tomography
Physiological Measurement **27**, pp. S43-S50

Isaacson D, Mueller J L, Newell J and Siltanen S 2004

Reconstructions of chest phantoms by the d-bar method for electrical impedance tomography
IEEE Transactions on Medical Imaging **23**(7), pp. 821-828

Knudsen K, Mueller J L and Siltanen S 2004

Numerical solution method for the dbar-equation in the plane
Journal of Computational Physics **198**(2), pp. 500-517

Mueller J L and Siltanen S 2003

Direct reconstructions of conductivities from boundary measurements
SIAM Journal of Scientific Computation **24**(4), pp. 1232-1266

Siltanen S, Mueller J L and Isaacson D 2000

An implementation of the reconstruction algorithm of A. Nachman for the 2-D inverse conductivity problem
Inverse Problems 16, pp. 681-699; *Erratum* Inverse problems **17** , pp. 1561-1563

This is a brief history of regularization methods for electrical impedance tomography

- 1991 **Hua, Woo, Webster** and **Tompkins** (Tikhonov and smoothness)
- 1992 **Goble, Cheney** and **Isaacson** (truncated Newton method)
- 1994 **Dobson** and **Santosa** (Total variation)
- 1999 **Vauhkonen** et al. (Tikhonov in 3D)
- 2001 **Kindermann** and **Neubauer** (surface representation)
- 2001 **Rondi** and **Santosa** (Mumford-Shah-functional)
- 2003 **Lukaschewitsch, Maass** and **Pidcock** (Tikhonov regularization)
- 2005 **Chung, Chan** and **Tai** (level set, total variation)
- 2005 **Eppler** and **Harbrecht** (Newton regularization)
- 2006 **Lechleiter** and **Rieder** (numerical Newton regularization)
- 2008 **Rondi** (theory for regularized recovery of discontinuities)
- 2008 **Lechleiter** and **Rieder** (local convergence of Newton regularization)